



UDC 533.6.011, 662.612, 517.95

PACS 47.70.Nd, 82.20.-w, 02.60.Lj,

DOI: 10.22363/2658-4670-2025-33-2-184-198

EDN: BPOFHS

Interval models of nonequilibrium physicochemical processes

Alexander Yu. Morozov^{1,2}, Dmitry L. Reviznikov^{1,2}, Vladimir Yu. Gidaspov²

¹ Federal Research Center Computer Science and Control of the Russian Academy of Sciences, 44-2 Vavilova St, Moscow, 119333, Russian Federation

² Moscow Aviation Institute (National Research University), 4 Volokolamskoe Highway, Moscow, 125993, Russian Federation

(received: November 15, 2024; revised: December 20, 2024; accepted: January 10, 2025)

Abstract. The paper discusses the application of the adaptive interpolation algorithm to problems of chemical kinetics and gas dynamics with interval uncertainties in reaction rate constants. The values of the functions describing the reaction rate may differ considerably if they have been obtained by different researchers. The difference may reach tens or hundreds of times. Interval uncertainties are proposed to account for these differences in models. Such problems with interval parameters are solved using the previously developed adaptive interpolation algorithm. On the example of modelling the combustion of a hydrogen-oxygen mixture, the effect of uncertainties on the reaction process is demonstrated. One-dimensional nonequilibrium flow in a rocket engine nozzle with different nozzle shapes, including a nozzle with two constrictions, in which a standing detonation wave can arise, is simulated. A numerical study of the effect of uncertainties on the structure of the detonation wave, as well as on steady-state flow parameters, such as the ignition delay time and the concentration of harmful substances at the nozzle exit, is performed.

Key words and phrases: chemical kinetics, gas dynamics, interval parameters, interval velocity constants, nozzle, rocket engine, standing detonation wave, adaptive interpolation algorithm

For citation: Morozov, A. Y., Reviznikov, D. L., Gidaspov, V. Y. Interval models of nonequilibrium physicochemical processes. *Discrete and Continuous Models and Applied Computational Science* **33** (2), 184–198. doi: 10.22363/2658-4670-2025-33-2-184-198. edn: BPOFHS (2025).

1. Introduction

In order to simulate gas-phase chemical transformations it is necessary to know the kinetic mechanism and the rates of the reactions taking place. As a rule, the dependences that describe the rates are obtained experimentally, often giving only approximate values [1]. The values of the functions approximating the rate of the same reaction, but obtained by different researchers, may differ by tens or hundreds of times. To account for these differences, we propose to use the interval apparatus [2–5]. In this case interval parameters are introduced into the model and simulation results are interval estimates for the values of interest.

© 2025 Morozov, A. Y., Reviznikov, D. L., Gidaspov, V. Y.



This work is licensed under a Creative Commons “Attribution-NonCommercial 4.0 International” license.

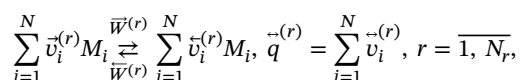
The previously developed adaptive interpolation algorithm [6–9] is used to solve such problems with interval parameters. The algorithm belongs to the methods that determine an explicit dependence of the solution of the problem on the values of interval parameters. Two subgroups can be distinguished in this group: methods using symbolic expressions [10–12] and methods representing the solution as a polynomial with respect to interval parameters [13, 14]. The adaptive interpolation algorithm belongs to the latter subgroup.

This algorithm has a theoretical justification. It consists in constructing a polynomial for each moment of time which interpolates the dependence of the problem solution on the values of the parameters in a given area of uncertainty. The interpolation polynomial is constructed on the basis of a set of nodes that form a grid. At each step of the algorithm, values in the nodes of the grid are updated, and then adaptation is made depending on the interpolation error. New nodes are added in places with a large error, and nodes are removed in places with a small error. The classical version of the algorithm uses interpolation on complete meshes, which limits its application to systems with a small number of interval parameters. However, two approaches, sparse meshes [15–17] and tensor trains [18, 19], have been applied in [20–22], which extend the application of the algorithm to dynamic systems with a large number of interval parameters.

The paper deals with the problems of chemical kinetics and gas dynamics. The simulation of combustion of a mixture of hydrogen and oxygen in the presence of interval uncertainties in the reaction rate constants has been carried out. A one-dimensional mathematical model describing chemical nonequilibrium flows in a nozzle of a given shape with uncertainties in the reaction rate constants is presented. Results of a numerical study of the effect of uncertainties on the structure of the detonation wave, as well as on steady-state flow parameters, such as the ignition delay time and the concentration of harmful substances at the nozzle exit, are presented.

2. Model of chemical kinetics

Here is a description of the basic relations. A multicomponent system of a variable composition of N substances, in which N_r reactions takes place, has the form [23]:



where M_i — symbols for molecules or atoms of chemical components, $\vec{q}^{(r)}$ — molecularity of elementary reactions, r — ordinal number of reaction, $\vec{v}_i^{(r)}$ — stoichiometric coefficients, $\vec{W}^{(r)}$ — the forward and reverse r -reaction rates.

The rate $\vec{W}^{(r)}$ is defined as the product of the reaction rate constant $\vec{K}^{(r)}(T)$ and the volume concentrations of the components:

$$\vec{W}^{(r)} = \vec{K}^{(r)}(T) \prod_i (\rho \gamma_i)^{\vec{v}_i^{(r)}},$$

where γ_i — molar-mass concentration of the i -th component, ρ — density.

The temperature dependence of the direct reaction rate constant is approximated by the generalised Arrhenius formula:

$$\vec{K}(T) = AT^n \exp\left(-\frac{E}{T}\right),$$

where A , n , E — some constant values for each specific reaction. It is in these quantities that the uncertainty may be contained.

The rate constants of reverse reactions are calculated using the equilibrium constant:

$$\tilde{K}^{(r)}(T) = \vec{K}^{(r)}(T) \exp \left[\sum_{i=1}^N (\tilde{v}_i^{(r)} - \vec{v}_i^{(r)}) \left(\frac{G_i^0(T)}{RT} + \ln \frac{RT}{P_0} \right) \right],$$

where $G_i^0(T)$ — the standard molar Gibbs potential of the i -component, which is given by using polynomials from the handbook [24], R — universal gas constant, $P_0 = 101325$ Pa — standard pressure.

The rate of formation of the i -component is as follows:

$$W_i = \sum_{r=1}^{N_r} (\vec{v}_i^{(r)} - \tilde{v}_i^{(r)}) (\vec{W}^{(r)} - \vec{W}^{(r)}), i = \overline{1, N}.$$

All thermodynamic quantities for a mixture of ideal gases are expressed in terms of the standard Gibbs molar potential. Here are some basic relations:

- Specific Gibbs potential: $G(T, P, \vec{\gamma}) = \sum_{i=1}^N \gamma_i \left[G_i^0(T) + RT \ln \left(P \gamma_i / P_0 \sum_{j=1}^N \gamma_j \right) \right];$
- Entropy: $S(T, P, \vec{\gamma}) = \sum_{i=1}^N \gamma_i \left[-\frac{dG_i^0(T)}{dT} - R \ln \left(P \gamma_i / P_0 \sum_{j=1}^N \gamma_j \right) \right];$
- Enthalpy (caloric equation): $H(T, \vec{\gamma}) = \sum_{i=1}^N \gamma_i \left(G_i^0(T) - T \frac{dG_i^0(T)}{dT} \right);$
- Internal energy (caloric equation): $U(T, \vec{\gamma}) = H(T, \vec{\gamma}) - RT \sum_{i=1}^N \gamma_i;$
- Isobaric heat capacity: $C_p(T, \vec{\gamma}) = \frac{\partial H(T, \vec{\gamma})}{\partial T};$
- Molar heat capacity: $C_v(T, \vec{\gamma}) = C_p(T, \vec{\gamma}) - R \sum_{i=1}^N \gamma_i;$
- Specific heat ratio: $\kappa(T, \vec{\gamma}) = \frac{C_p(T, \vec{\gamma})}{C_v(T, \vec{\gamma})};$
- Sound speed: $a(T, \vec{\gamma}) = \sqrt{\kappa(T, \vec{\gamma}) RT \sum_{i=1}^N \gamma_i};$
- Equation of state for a mixture of ideal gases (thermal equation):

$$P = \rho RT \sum_{i=1}^N \gamma_i;$$

where $\vec{\gamma} = (\gamma_1, \gamma_2, \dots, \gamma_N)$.

The kinetic mechanisms from [25] (table 1) and [26] (table 2) have been considered to demonstrate the uncertainties associated with the rate constants of chemical reactions. The equilibrium constant was used to compare the reactions. Figure 1 shows the temperature dependences of the rate constants for different mechanisms in accordance with [20]. The strongest mismatch of the curves is observed for reactions 1, 3 and 8 from mechanism 2 which was taken into account in the corresponding interval coefficients (table 3).

Thus, the value in the Arrhenius formula becomes interval, and as a consequence the temperature dependence of the rate constants also becomes interval.

Table 1

The first combustion mechanism of the mixture $H_2 - O_2$

№	Reaction	A, m, mol, s	n	E, K
1.	$O_2 + H \rightarrow OH + O$	2.0×10^8	0.0	8455
2.	$H_2 + O \rightarrow OH + H$	5.06×10^{-2}	2.67	3163
3.	$H_2 + OH \rightarrow H_2O + H$	1.0×10^2	1.6	1659
4.	$OH + OH \rightarrow H_2O + O$	1.5×10^3	1.14	50
5.	$H + H + M \rightarrow H_2 + M$	1.8×10^6	-1.0	0
6.	$O + O + M \rightarrow O_2 + M$	2.9×10^5	-1.0	0
7.	$H + OH + M \rightarrow H_2O + M$	2.2×10^{10}	-2.0	0

Table 2

The second combustion mechanism of the mixture $H_2 - O_2$

№	Reaction	A, m, mol, s	n	E, K
1.	$H_2O + H \rightarrow OH + H_2$	8.4×10^7	0	10116
2.	$O_2 + H \rightarrow OH + O$	2.2×10^8	0	8455
3.	$H_2 + O \rightarrow OH + H$	1.8×10^4	1	4480
4.	$O_2 + M \rightarrow 2O + M$	5.4×10^{12}	-1	59400
5.	$H_2 + M \rightarrow 2H + M$	2.2×10^8	0	48300
6.	$H_2O + M \rightarrow OH + H + M$	10^{18}	-2.2	59000
7.	$HO + M \rightarrow O + H + M$	8.5×10^{12}	-1	50830
8.	$H_2O + O \rightarrow 2OH$	5.8×10^7	0	9059

Table 3

The interval part of the mixture combustion mechanism $H_2 - O_2$

№	Reaction	A, m, mol, s	n	E, K
1.	$H_2O + H \rightarrow OH + H_2$	$[8.4 \times 10^7, 4.2 \times 10^8]$	0	10116
3.	$H_2 + O \rightarrow OH + H$	$[1.8 \times 10^4, 9 \times 10^4]$	1	4480
8.	$H_2O + O \rightarrow 2OH$	$[5.8 \times 10^7, 2.9 \times 10^8]$	0	9059

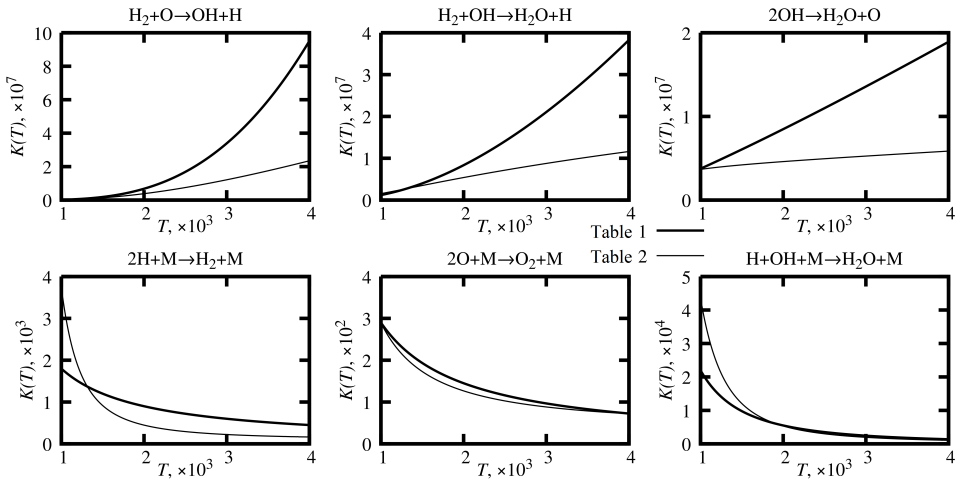


Figure 1. Comparison of different mixture combustion mechanisms $\text{H}_2 - \text{O}_2$

Let us simulate the combustion of a mixture of hydrogen and oxygen in the presence of uncertainties in the reaction rate constants according to [20]. Consider a stoichiometric mixture of hydrogen and oxygen at initial temperature $T = 1200$ K, constant density $\rho = 0.122$ kg / m³ and constant internal energy $U = 1.48$ MJ / kg. A chemical kinetics model is given by a system of six components (H_2O , OH , H_2 , O_2 , H , O) in which eight reactions occur (table 2 and table 3). Here, the ODE system is written as follows:

$$\frac{d\gamma_i}{dt} = \frac{1}{\rho} \sum_{r=1}^{N_r} (\vec{v}_i^{(r)} - \vec{v}_i^{(r)}) (\vec{W}^{(r)} - \vec{W}^{(r)}), \quad i = \overline{1, N}$$

— and is complemented by the equation of conservation of internal energy of the system:

$$U(T, \vec{\gamma}) = H(T, \vec{\gamma}) - RT \sum_{j=1}^N \gamma_j.$$

For each calculation of the right-hand side of the ODE system, the internal energy equation is solved relatively T using Newton's method.

Initial conditions: $\gamma_{\text{H}_2} = 55.50868$ mol / kg, $\gamma_{\text{O}_2} = 27.75434$ mol / kg, $\gamma_{\text{H}_2\text{O}} = \gamma_{\text{OH}} = \gamma_{\text{H}} = \gamma_{\text{O}} = 0$ mol / kg.

To integrate the resulting rigid ODE system, the implicit Rosenbrock method with a frozen Jacobi matrix was used [27]. Figure 2 shows the upper and lower estimates of the concentrations of all components in the mixture. The uncertainty in the reaction rate constants leads to an uncertainty in the ignition delay time between 22 and 29 μs .

Note that in this model the equilibrium state is reached regardless of the values of the reaction rate constants. This is confirmed by the fact that after a certain point in time, the upper estimates of the concentrations coincide with the lower estimates. In addition, note that the results obtained are in agreement with those obtained earlier in [20], in which the differences in the above kinetic mechanisms were accounted for in a different way.

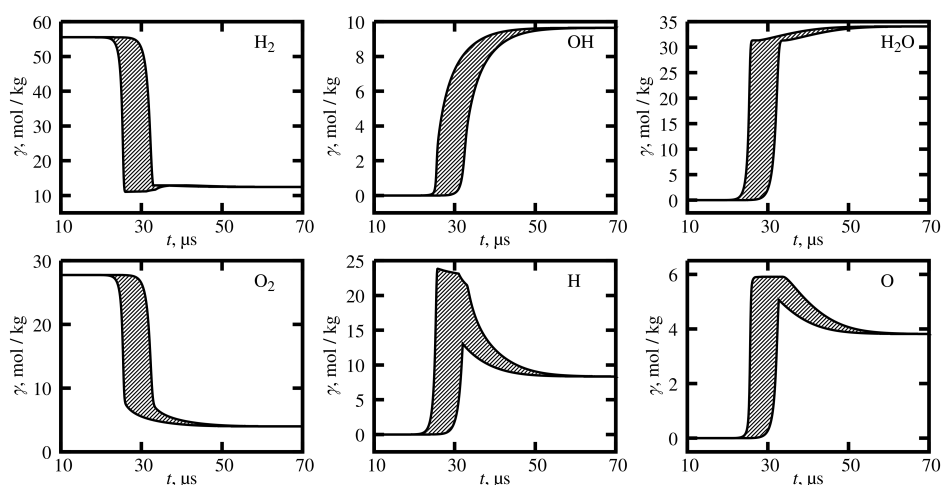


Figure 2. Dependence of mole-mass concentrations on time

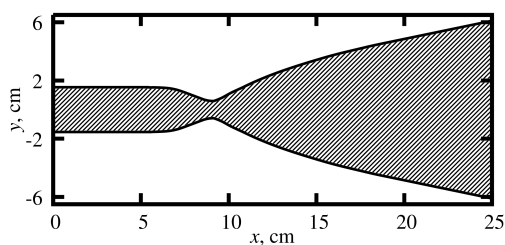


Figure 3. Nozzle profile

3. Chemical non-equilibrium flow in a nozzle

When simulating the flow in a liquid rocket engine (LRE) nozzle, ambiguity in the kinetic constants leads to uncertainties in all macro-parameters, such as thrust, Mach number, etc. Also the parameters of freezing values of concentrations of toxic combustion products become ambiguous, which is important from the point of view of ecology. For such problems, it is a natural need to determine interval estimates of solutions from known interval values of initial data. In practice, the simulation of the flow in an LRE nozzle is reduced to solving rigid ODE systems, which can be reintegrated by an adaptive interpolation algorithm.

A one-dimensional flow in the nozzle of a liquid rocket engine (figure 3) running on asymmetric dimethylhydrazine $(\text{CH}_3)_2\text{N}_2\text{H}_2$ and nitrogen tetroxide N_2O_4 is considered. The pressure in the combustion chamber is $P = 100$ atm, the oxidant excess ratio is $\alpha = 1$, the enthalpy is $H = 42.57$ kJ/kg. The concentrations in the combustion chamber were calculated from the condition of chemical equilibrium. The chemical processes were modelled by kinetic mechanism[28] involving 15 reactions and where 12 components are participating (table 4). Interval uncertainties were introduced in the rates of reactions 1 and 15.

Kinetic mechanism for the system C-O-H-N

Table 4

№	Reaction	A, m, mol, s	n	E , kJ / mol
1.	$\text{CO} + \text{O} + \text{M} \leftrightarrow \text{CO}_2 + \text{M}$	$[3.5 \times 10^2, 3.5 \times 10^3]$	0	1.06
2.	$\text{OH} + \text{H} + \text{M} \leftrightarrow \text{H}_2\text{O} + \text{M}$	1.2×10^8	−1	0
3.	$\text{O} + \text{N} + \text{M} \leftrightarrow \text{NO} + \text{M}$	3.3×10^3	0	0
4.	$\text{H} + \text{H} + \text{M} \leftrightarrow \text{H}_2 + \text{M}$	1.4×10^8	−1.5	0
5.	$\text{O} + \text{O} + \text{M} \leftrightarrow \text{O}_2 + \text{M}$	5.5×10^5	−0.87	0
6.	$\text{N} + \text{N} + \text{M} \leftrightarrow \text{N}_2 + \text{M}$	2.7×10^4	−0.5	0
7.	$\text{H} + \text{O} + \text{M} \leftrightarrow \text{OH} + \text{M}$	3.3×10^6	−0.5	0
8.	$\text{H}_2 + \text{OH} \leftrightarrow \text{H}_2\text{O} + \text{H}$	1.1×10^8	0	4.33
9.	$\text{H}_2 + \text{O} \leftrightarrow \text{OH} + \text{H}$	1.3×10^7	0	4.96
10.	$\text{O}_2 + \text{H} \leftrightarrow \text{OH} + \text{O}$	2.2×10^8	0	8.3
11.	$\text{O}_2 + \text{N}_2 \leftrightarrow \text{NO} + \text{NO}$	5.2×10^7	0	53.85
12.	$\text{NO} + \text{N} \leftrightarrow \text{N}_2 + \text{O}$	3×10^7	0	0.1
13.	$\text{NO} + \text{O} \leftrightarrow \text{O}_2 + \text{N}$	1.1×10^7	0	20.97
14.	$\text{OH} + \text{OH} \leftrightarrow \text{H}_2\text{O} + \text{O}$	1.0×10^7	0	0.6
15.	$\text{CO} + \text{OH} \leftrightarrow \text{CO}_2 + \text{H}$	$[2.5 \times 10^6, 2.5 \times 10^7]$	0	2.57

Gas flow without viscosity, thermal conductivity and diffusion is considered. Such gas flows in channels with gentle walls in continuous flow regions are given by equations which have the following divergent form:

$$\left\{\begin{aligned} \frac{\partial}{\partial t}\rho F + \frac{\partial}{\partial x}\rho u F &= 0, \\ \frac{\partial}{\partial t}\rho u F + \frac{\partial}{\partial x}(\rho u^2 + P) F &= P \frac{\partial F}{\partial x}, \\ \frac{\partial}{\partial t}\rho \left(e + \frac{u^2}{2}\right) F + \frac{\partial}{\partial x}\rho u \left(e + \frac{P}{\rho} + \frac{u^2}{2}\right) F &= 0, \\ \frac{\partial}{\partial t}\rho \gamma_i F + \frac{\partial}{\partial x}\rho u \gamma_i F &= F W_i, \quad i = \overline{1, N}. \end{aligned}\right.$$

$$\left\{\begin{aligned} W_i &= \sum_{r=1}^{N_r} \left(\bar{v}_i^{(r)} - \bar{v}_i^{(r)}\right) \left(\bar{W}^{(r)} - \bar{W}^{(r)}\right), \\ \bar{W}^{(r)} &= \bar{K}^{(r)}(T) \prod_i (\rho \gamma_i)^{\bar{v}_i^{(r)}}, \\ \bar{K}(T) &= A T^n \exp\left(-\frac{E}{T}\right). \end{aligned}\right.$$

Here first three equations are equations of conservation of mass (continuity), momentum and energy respectively; last equations are equations describing change of chemical composition; $F = F(x)$ - dependence of channel area on longitudinal coordinate; N - number of components in mixture. The system of equations is closed by thermal and caloric equations of state: $\rho = \rho(T, P, \bar{\gamma})$, $e = e(T, P, \bar{\gamma})$.

The finite volume method with TVD monotonization was used for modeling the flow, and the Harten-Lax-van Leer scheme was used for calculations of flows through cell boundaries. Since the resulting ODE system is rigid, it was integrated in two steps: at each step of the Runge-Kutta second-order method, which integrated the gas-dynamic equations, several steps were performed by the

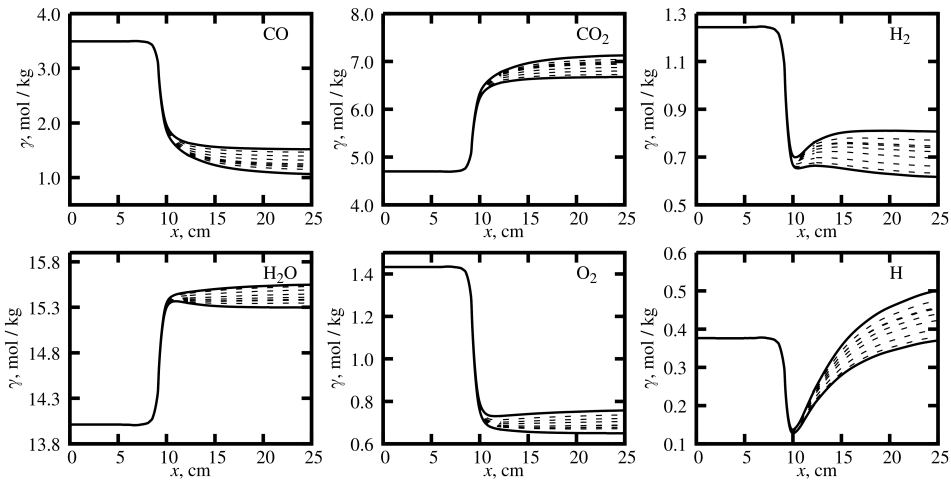


Figure 4. Mole-mass concentration distribution of the components in the nozzle

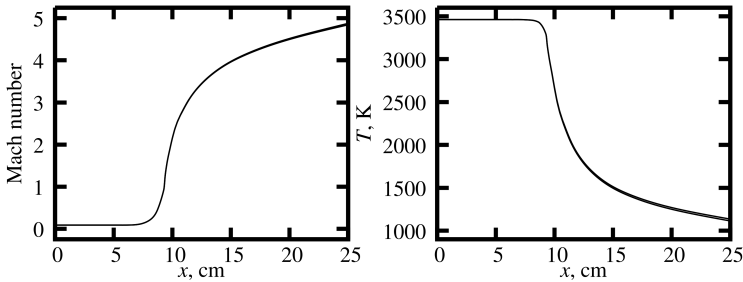


Figure 5. Macroparameter distribution in the nozzle

implicit Rosenbrock method with a frozen Jacobi matrix to integrate the chemical kinetics equations in each cell.

Figure 4 shows the concentration distributions of some mixture components in the nozzle after the flow has been established. Uncertainties in the reaction rate constants affect the freezing of the mixture components, which in turn affects the environmental performance of the engine. The dashed lines in this figure show a number of Monte Carlo runs. These are all contained in the resulting estimates. Figure 5 shows the interval estimates of the macro parameters.

Unlike concentrations, uncertainties in rate constants have much less effect on Mach number, temperature, pressure, etc.

4. Standing detonation wave

According to classical theory, a detonation wave (DW) propagating through an explosive mixture is a combination of a shock wave (SW) and an adjacent thin zone in which exothermic chemical reactions take place, ending in chemical equilibrium, with the zone of chemical transformations propagating at the SW.

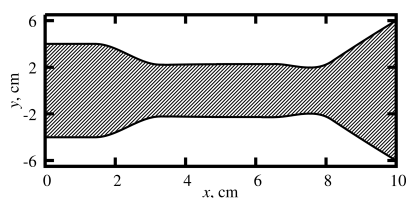


Figure 6. Nozzle profile with two constrictions

In this section, we consider one-dimensional supersonic flow in a nozzle, which is characterized by the occurrence of a standing detonation wave. Of interest is the case when a standing DW is realized up to the critical section (CS) and then the flow accelerates again to supersonic velocity at the transition through the CS. According to the classical theory [29], standing DW in the narrowing part of the channel is unstable, so for its long-term stable existence the nozzle shape with two constrictions is used. Mathematical model is a system of equations written in the previous section.

First consider a nozzle shape in which the first contraction is weakly pronounced (figure 6). The range in which the radius at the expansion section is located is chosen from the solution of the corresponding steady-state equilibrium problem. In this range a standing DW is guaranteed, assuming that all chemical transformations occur infinitely fast. In the previous problem it was obtained that the uncertainties in the reaction rate constants affect the macro parameters insignificantly, and in order to enhance their effect, the section of the nozzle where the DW should be established is made very shallow.

A mixture of H_2 , O_2 , N_2 , Ar is fed to the nozzle inlet with velocity $u = 2750 \text{ m/s}$, pressure $P = 1 \text{ atm}$ and temperature $T = 400 \text{ K}$ in the ratio 42 : 21 : 78 : 1 [30]. Four interval uncertainties are introduced into the kinetic mechanism (table 5), which slow down the corresponding reactions by a hundred thousand times.

The flow establishment was carried out in several stages. In the first stage, only supersonic flow of unreacted gas was obtained. In the second stage, a SW was artificially induced. At the moment when it was at the required section of the nozzle, the non-interval kinetic mechanism was engaged. In the third stage, after a standing DW had been established, the interval kinetic mechanism was used.

Figure 7 shows the distributions of component concentrations in the nozzle. The presence of uncertainties in the kinetic mechanism strongly affected the width of the interval concentration estimates, in contrast to the width of the temperature estimates (figure 8). The concentration spikes in the last three plots are not anomalous and are explained by the fact that basically all chemical transformations take place in the DW region.

The following example takes a closer look at the structure of the standing DW and how it is affected by small uncertainties in the reaction rate constants. As before, a nozzle with two constrictions is used here (figure 9) and the same mixture of H_2 , O_2 , N_2 , Ar is fed to the inlet of the nozzle.

At the point where the DW is roughly to be established, a strong compaction of the computational grid is performed so that the DW can be considered in detail. Given the constructed spatial grid, the resulting ODE system contains over 30,000 equations. The nozzle inlet velocity $u = 2500 \text{ m/s}$, pressure $P = 1.38 \text{ atm}$ and temperature $T = 391 \text{ K}$. We replace the four interval coefficients in table 5 with two according to table 6. Figure 10 shows the distributions of the interval estimates of the concentrations of all substances in the nozzle in the vicinity of the standing DW for several substances.

Figure 11 shows the distribution of Mach number and temperature in the nozzle. Practically invisible, both temperature and Mach number are interval.

Table 5

Kinetic mechanism for the system $H_2 - O_2$

№	Reaction	A, m, mol, s	n	E, K
1.	$H_2O + H \leftrightarrow OH + H_2$	$[8.4 \times 10^2, 8.4 \times 10^7]$	0	10116
2.	$O_2 + H \leftrightarrow OH + O$	$[2.2 \times 10^3, 2.2 \times 10^8]$	0	8455
3.	$H_2 + O \leftrightarrow OH + H$	1.8×10^4	1	4480
4.	$O_2 + M \leftrightarrow 2O + M$	5.4×10^{12}	-1	59400
5.	$H_2 + M \leftrightarrow 2H + M$	2.2×10^8	0	48300
6.	$H_2O + M \leftrightarrow OH + H + M$	$[1 \times 10^{13}, 1 \times 10^{18}]$	-2.2	59000
7.	$HO + M \leftrightarrow O + H + M$	8.5×10^{12}	-1	50830
8.	$H_2O + M \leftrightarrow 2OH$	$[5.8 \times 10^2, 5.8 \times 10^7]$	0	9059
9.	$H + O_2 + M \leftrightarrow HO_2 + M$	3.5×10^4	-0.41	-565
10.	$H_2 + O_2 \leftrightarrow H + HO_2$	7.39×10^{-1}	0.6	26926
11.	$H_2O + O \leftrightarrow H + HO_2$	4.76×10^5	2.43	28743
12.	$H_2O + O_2 \leftrightarrow OH + HO_2$	1.5×10^9	0.372	36600
13.	$2OH \leftrightarrow H + HO_2$	1.2×10^7	0.5	20200
14.	$OH + O_2 \leftrightarrow O + HO_2$	1.3×10^7	0	28200
15.	$H + H_2O_2 \leftrightarrow H_2 + HO_2$	1.6×10^6	0	1900
16.	$H + H_2O_2 \leftrightarrow H_2O + OH$	5×10^8	0	5000
17.	$2HO_2 \leftrightarrow H_2O_2 + O_2$	1.8×10^7	0	500
18.	$HO_2 + H_2O \leftrightarrow H_2O_2 + OH$	1.8×10^7	0	15100
19.	$OH + HO_2 \leftrightarrow H_2O_2 + O$	5.2×10^4	0.5	10600

Table 6

The modified reaction coefficients from table 5

№	Reaction	A, m, mol, s	n	E, K
1.	$H_2O + H \leftrightarrow OH + H_2$	8.4×10^7	0	10116
2.	$O_2 + H \leftrightarrow OH + O$	2.2×10^8	0	8455
6.	$H_2O + M \leftrightarrow OH + H + M$	1×10^{18}	-2.2	59000
8.	$H_2O + M \leftrightarrow 2OH$	5.8×10^7	0	9059
16.	$H + H_2O_2 \leftrightarrow H_2O + OH$	$[2.5 \times 10^8, 5 \times 10^8]$	0	5000
19.	$OH + HO_2 \leftrightarrow H_2O_2 + O$	$[5.2 \times 10^4, 2.6 \times 10^5]$	0.5	10600

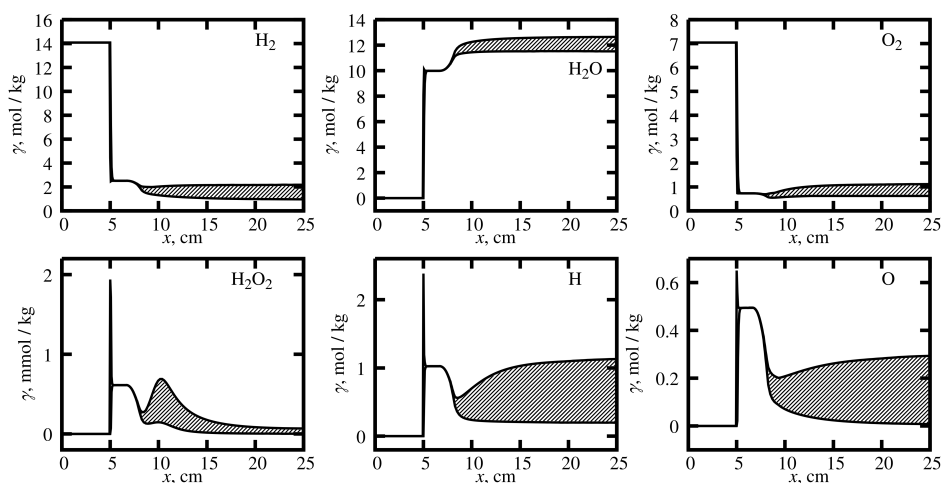


Figure 7. Mole-mass concentration distribution of the components in the nozzle

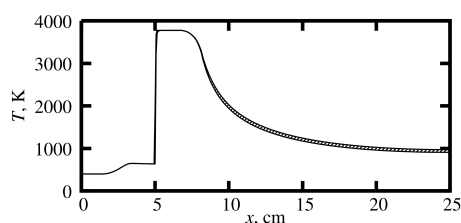


Figure 8. Temperature distribution in the nozzle

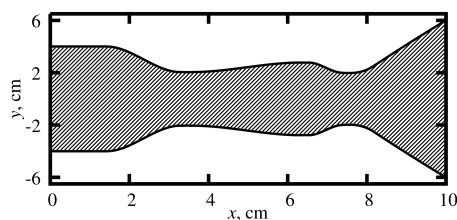


Figure 9. Nozzle profile with two pronounced constrictions

When the x-axis is zoomed in 2500 times (inset in the graphs), the structure of the DW becomes visible. The temperature plot clearly shows the SW followed by a zone of exothermic chemical reactions. Here there is a slight shift of the DV front and a slight increase in the ignition delay time.

5. Conclusion

A simulation of combustion of a hydrogen-oxygen mixture in the presence of uncertainties in the reaction rate constants has been carried out. A mathematical model of nonequilibrium flows has been developed, taking into account uncertainties in the values of reaction rate constants. Numerical studies of the effect of uncertainties on the structure of the detonation wave, as well as on the parameters of the steady-state flow, such as the ignition delay time and the concentration of harmful substances at the nozzle exit, have been performed. It is obtained that the uncertainties mainly affect the chemical composition at the nozzle exit and, to a lesser extent, the temperature, Mach number, and detonation wave. All obtained results do not contradict the already known solutions and coincide with the solutions obtained by the Monte Carlo method. The solved problems further confirm the efficiency and universality of the adaptive interpolation algorithm developed earlier

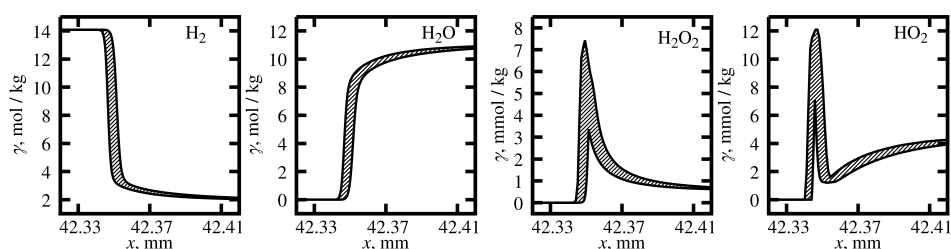


Figure 10. Distribution of component concentrations in the standing DW region

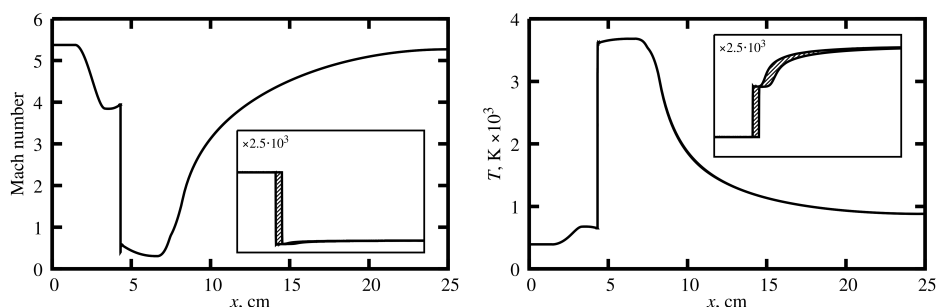


Figure 11. Mach number and temperature distribution in the standing DV region

Author Contributions: Methodology, software, investigation, A.Yu.M.; conceptualization, methodology, supervision, D.L.R.; methodology, validation, V.Yu.G. All authors have read and agreed to the published version of the manuscript.

Funding: This research received no external funding.

Data Availability Statement: Data sharing not applicable.

Conflicts of Interest: The authors declare no conflict of interest.

References

1. Vaitiev, V. A. & Mustafina, S. A. Searching for uncertainty regions of kinetic parameters in the mathematical models of chemical kinetics based on interval arithmetic. Russian. *Bulletin of the South Ural State University. Series Mathematical Modelling, Programming & Computer Software* **7**, 99–110. doi:10.14529/mmp140209 (2014).
2. Moore, R. E. *Interval analysis* 145 pp. (Prentice-Hall, New Jersey, Englewood Cliffs, 1966).
3. Moore, R. E., Kearfott, R. B. & Cloud, M. J. *Introduction to Interval Analysis* 223 pp. doi:10.1137/1.9780898717716 (Society for Industrial and Applied Mathematics, 2009).
4. Bazhenov, A. N., Zhilin, S. I., Kumkov, S. I. & Shary, S. P. *Processing and analysis of interval data* Russian. 356 pp. (Institute of Computer Research, Izhevsk, 2024).
5. Dobronec, B. S. *Interval mathematics* Russian. 287 pp. (SibFU, Krasnoyarsk, 2007).
6. Morozov, A. Y. & Reviznikov, D. L. Adaptive Interpolation Algorithm Based on a kd-Tree for Numerical Integration of Systems of Ordinary Differential Equations with Interval Initial Conditions. *Differential Equations* **54**, 945–956. doi:10.1134/S0012266118070121 (2018).

7. Morozov, A. Y. & Reviznikov, D. L. Adaptive sparse grids with nonlinear basis in interval problems for dynamical systems. *Computation* **11**. doi:10.3390/computation11080149 (2023).
8. Morozov, A. Y., Zhuravlev, A. A. & Reviznikov, D. L. Analysis and Optimization of an Adaptive Interpolation Algorithm for the Numerical Solution of a System of Ordinary Differential Equations with Interval Parameters. *Differential Equations* **56**, 935–949. doi:10.1134/s0012266120070125 (2020).
9. Morozov, A. Y., Reviznikov, D. L. & Gidaspov, V. Y. Adaptive Interpolation Algorithm Based on a KD-Tree for the Problems of Chemical Kinetics with Interval Parameters. *Mathematical Models and Computer Simulations* **11**, 622–633. doi:10.1134/S2070048219040100 (2019).
10. Makino, K. & Berz, M. *Verified Computations Using Taylor Models and Their Applications in Numerical Software Verification* **10381** (Springer International Publishing, Heidelberg, Germany, July 22–23, 2017), 3–13. doi:10.1007/978-3-319-63501-9_1.
11. Neher, M., Jackson, K. & Nedialkov, N. On Taylor model based integration of ODEs. *SIAM Journal on Numerical Analysis* **45**, 236–262. doi:10.1137/050638448 (2007).
12. Rogalev, A. N. Guaranteed Methods of Ordinary Differential Equations Solution on the Basis of Transformation of Analytical Formulas. Russian. *Computational technologies* **8**, 102–116 (2003).
13. Fu, C., Ren, X., Yang, Y., Lu, K. & Qin, W. Steady-state response analysis of cracked rotors with uncertain-but-bounded para-meters using a polynomial surrogate method. *Communications in Nonlinear Science and Numerical Simulation* **68**, 240–256. doi:10.1016/j.cnsns.2018.08.004 (2018).
14. Fu, C., Xu, Y., Yang, Y., Lu, K., Gu, F. & Ball, A. Response analysis of an accelerating unbalanced rotating system with both random and interval variables. *Journal of Sound and Vibration* **466**. doi:10.1016/j.jsv.2019.115047 (2020).
15. Smoliak, S. A. Quadrature and Interpolation Formulae on Tensor Products of Certain Classes of Functions. Russian. *Dokl. Akad. Nauk. Ssr* **148**, 1042–1045 (1963).
16. Bungartz, H.-J. & Griebel, M. Sparse grids. *Acta Numerica* **13**, 147–269 (2004).
17. Bungartz, H. J. *Finite Elements of Higher Order on Sparse Grids* 127 pp. (Shaker Verlag, Germany, Duren/Maastricht, 1998).
18. Oseledets, I. V. Tensor-train decomposition. *SIAM Journal on Scientific Computing* **33**, 2295–2317. doi:10.1137/090752286 (2011).
19. Oseledets, I. & Tyrtysnikov, E. TT-cross approximation for multidimensional arrays. *Linear Algebra and its Applications* **432**, 70–88. doi:10.1016/j.laa.2009.07.024 (2010).
20. Gidaspov, V. Y., Morozov, A. Y. & Reviznikov, D. L. Adaptive Interpolation Algorithm Using TT-Decomposition for Modeling Dynamical Systems with Interval Parameters. *Computational Mathematics and Mathematical Physics* **61**, 1387–1400. doi:10.1134/S0965542521090098 (2021).
21. Morozov, A. Y., Zhuravlev, A. A. & Reviznikov, D. L. Sparse Grid Adaptive Interpolation in Problems of Modeling Dynamic Systems with Interval Parameters. *Mathematics* **9**. doi:10.3390/math9040298 (2021).
22. Morozov, A. & Reviznikov, D. Adaptive Interpolation Algorithm on Sparse Meshes for Numerical Integration of Systems of Ordinary Differential Equations with Interval Uncertainties. *Differential Equations* **57**, 947–958. doi:10.1134/S0012266121070107 (2021).
23. Gidaspov, V. Y. & Severina, N. S. *Elementary Models and Computational Algorithms in Physical Fluid Dynamics. Thermodynamica and Chemical Kinetics* Russian. 84 pp. (Faktorial, Moscow, 2014).
24. Glushko, V. P., Gurvich, L. V., Veits, I. V. & et al. *Thermodynamic Properties of Some Substances* Russian (Nauka, Moscow, 1978).
25. Warnatz, J., Maas, U. & Dibble, R. *Combustion. Physical and Chemical Fundamentals, Modelling and Simulation, Experiments, Pollutant Formation* 378 pp. doi:10.1007/978-3-540-45363-5 (Springer, Berlin, Heidelberg, 2006).

26. Starik, A. M., Titova, N. S., Sharipov, A. S. & Kozlov, V. E. Syngas oxidation mechanism. *Combustion, Explosion, and Shock Waves* **46**, 491–506. doi:10.1007/s10573-010-0065-x (2010).
27. Novikov, E. A. & Golushko, M. I. (m, 3) third-order method for stiff nonautonomous systems of ODEs. Russian. *Computational technologies* **3**, 48–54 (1998).
28. Pirumov, U. G. & Roslyakov, G. S. *Gas dynamics of nozzles* Russian. 368 pp. (Nauka, Moscow, 1990).
29. Cherny, G. G. *Gas dynamics* Russian. 424 pp. (Nauka, Moscow, 1988).
30. Zhuravskaya, T. A. & Levin, V. A. Stabilization of detonation combustion of a high-velocity combustible gas mixture flow in a plane channel. *Fluid Dynamics* **50**, 283–293. doi:10.1134/S001546281502012X (2015).

Information about the authors

Morozov, Alexander Yu.—Doctor of Physical and Mathematical Sciences, Senior Researcher, Department of Mathematical Modeling of Heterogeneous Systems, Federal Research Center Computer Science and Control of the Russian Academy of Sciences; Associate Professor of the Department of Computational Mathematics and Programming, Moscow Aviation Institute (National Research University) (e-mail: morozov@infway.ru, ORCID: 0000-0003-0364-8665, ResearcherID: ABC-7836-2021, Scopus Author ID: 57203389215)

Reviznikov, Dmitry L.—Doctor of Physical and Mathematical Sciences, Professor, Leading Researcher, Department of Mathematical Modeling of Heterogeneous Systems, Federal Research Center Computer Science and Control of the Russian Academy of Sciences; Professor of the Department of Computational Mathematics and Programming, Moscow Aviation Institute (National Research University) (e-mail: reviznikov@mai.ru, ORCID: 0000-0003-0998-7975, ResearcherID: T-4571-2018, Scopus Author ID: 6602701797)

Gidaspov, Vladimir Yu.—Doctor of Physical and Mathematical Sciences, Associate Professor, Professor of the Department of Computational Mathematics and Programming, Moscow Aviation Institute (National Research University) (e-mail: gidaspov@mai.ru, ORCID: 0000-0002-5119-4488, ResearcherID: B-4572-2019, Scopus Author ID: 6506396733)

УДК 533.6.011, 662.612, 517.95

PACS 47.70.Nd, 82.20.-w, 02.60.Lj,

DOI: 10.22363/2658-4670-2025-33-2-184-198

EDN: BPOFHS

Интервальные модели неравновесных физико-химических процессов

А. Ю. Морозов^{1,2}, Д. Л. Ревизников^{1,2}, В. Ю. Гидаспов²

¹ Федеральный исследовательский центр “Информатика и управление” Российской академии наук, ул. Вавилова, д. 44, кор. 2, Москва, 119333, Российская Федерация

² Московский авиационный институт (национальный исследовательский университет), Волоколамское шоссе, д. 4, Москва, 125993, Российская Федерация

Аннотация. В данной работе рассматривается применение алгоритма адаптивной интерполяции к задачам химической кинетики и газовой динамики с интервальными неопределенностями констант скоростей реакций. Значения функций, описывающих скорость реакции, могут значительно различаться, если они были получены разными исследователями. Разница может достигать десятков или сотен раз. Для учета данных различий в моделях предлагается использовать интервальные неопределенности. Решение таких задач с интервальными параметрами выполняется с помощью ранее разработанного алгоритма адаптивной интерполяции. На примере моделирования горения смеси водорода и кислорода демонстрируется влияние неопределенностей на процесс протекания реакций. Моделируется одномерное неравновесное течение в сопле ракетного двигателя с разной формой сопла, включая сопло с двумя сужениями, в котором может возникать стоячая детонационная волна. Выполняется численное исследование влияния неопределенностей на структуру детонационной волны, а так же на параметры установившегося течения, такие как время задержки воспламенения и концентрация вредных веществ на выходе из сопла.

Ключевые слова: химическая кинетика, газовая динамика, интервальные параметры, интервальные константы скоростей, сопло, ракетный двигатель, стоячая детонационная волна, алгоритм адаптивной интерполяции